Giant isotope effect on the itinerant-electron metamagnetism in $YFe_2(H_yD_{1-y})_{4.2}$

V. Paul-Boncour,[1,*] M. Guillot,[2] G. Wiesinger,[3] and G. André[4]
[1]*LCMTR, CNRS, 2 rue H. Dunant, 94320 Thiais Cedex, France*
[2]*LCMI, CNRS-MPI, BP166, 38042 Grenoble Cedex 9, France*
[3]*IFP, T.U. Wien, Wiedner Haupstrasse 8-10, 1040 Vienna, Austria*
[4]*LLB, CE-Saclay, 91191 Gif/Yvette, France*
(Received 1 July 2005; revised manuscript received 25 August 2005; published 30 November 2005)

The $YFe_2(H_yD_{1-y})_{4.2}$ compounds ($y=0, 0.64, 1$) crystallize in the same monoclinic structure with a linear increase of the cell volume reaching 0.80% between the hydride and the deuteride. These compounds undergo a first-order magnetovolumic transition from a ferromagnetic to an antiferromagnetic structure, which is related to an itinerant electron metamagnetism (IEM) transition of one of the Fe sites that is surrounded by about 5 (H, D) atoms. A large H/D isotope effect is observed on the magnetic properties: the hydride presents a larger spontaneous magnetization and a 50% higher transition temperature T_{M0} than the deuteride. This large isotope effect is attributed to the large cell volume difference between the hydride and the deuteride, which plays a dominant role due to the strong interplay between magnetic and elastic energy in IEM compounds.

DOI: 10.1103/PhysRevB.72.174430 PACS number(s): 75.50.Bb, 76.50.+g, 76.80.+y, 61.12.Ld

I. INTRODUCTION

The isotopic exchange of hydrogen (H) by a heavier isotope (D, T) is known to modify the thermodynamic properties of metal hydride systems, in particular, the enthalpy of formation and the hydrogen isotope solubility. For example, in pure Pd the equilibrium pressure decreases with increasing isotope mass,[1] while the opposite effect is observed for intermetallic compounds like $LaNi_5$, $SmCo_5$, ZrCo, $UZr_{0.29}$.[2–5]

Several studies have also revealed an isotope effect on the electronic properties of binary metal hydrides.[6] For example, there is a reverse isotope effect on the critical temperature T_C in superconducting Pd–H and Pd–D with an increase of T_C from 8 to 10 K.[6–8] Isotope effects were also observed in nuclear spin-lattice relaxation rates, changes of impurity resistivity due to hydrogen in Pd, Ta, or rare earth metals.[6,9] Such isotope effects on the electronic properties of metal hydrides have been related to the large amplitude of the zero-point vibration of hydrogen and the strong influence of the isotope mass, which gives rise to quantum effects.[6,10,11] The isotope mass has also a significant influence on physical properties related to the diffusion of the H isotope, like the magnetic aftereffect that is used to study ferromagnetic metals and alloys with a diluted hydrogen content[12] or structural transitions related to vacancy ordering in $ZrBe_2(H/D)_x$.[13]

It is generally assumed, however, that replacing hydrogen by deuterium in a ternary metal hydride does not modify significantly its structural and magnetic properties and that neutron diffraction results on deuterides can be used to determine the related hydride properties. It was therefore rather surprising to observe a very large isotope effect on the magnetic properties of the $YFe_2(H,D)_{4.2}$ system. In this system, replacing deuterium by hydrogen leads to a shift of a steep magnetovolumic transition from 90 to 140 K ($B=1.2$ T), i.e., an increase of nearly 50% of this transition temperature.[14] $YFe_2D_{4.2}$ crystallizes in a cubic structure above 345 K and undergoes a lowering of crystal symmetry from cubic to rhombohedral symmetry between 343 and 320 K, then from a rhombohedral to a monoclinic structure below 320 K due to deuterium order.[13] In order to understand the origin of this giant isotope effect on the magnetic properties, additional results obtained from $YFe_2(H_yD_{1-y})_{4.2}$ ($y=0, 0.64, 1$) compounds by x-ray and neutron powder diffraction, differential scanning calorimetry, high magnetic field magnetization measurements, and ^{57}Fe Mössbauer spectroscopy for $T \leqslant 300$ K will be presented. The analysis of the experimental results compared with other systems, showing a similar magnetic behavior, will indicate that the steep magnetovolumic transition can be related to an itinerant electron metamagnetic transition. Using both experimental and theoretical results, we will show that the giant isotope effect can be mainly attributed to the large volume change observed between the deuteride and the hydride.

II. EXPERIMENTAL

The preparation and the characterization of single phase YFe_2 and $YFe_2(H,D)_{4.2}$ compounds is described in Ref. 13. X-ray diffraction (XRD) measurements at 300 K were carried out using a Bruker D8 diffractometer (Cu K_α radiation). XRD measurements at low temperature were performed on a Bruker D8 diffractometer (Cu K_α radiation) equipped with a liquid nitrogen flow cryostat for $YFe_2H_{4.2}$ and with a Siemens D500 diffractometer (Co K_α radiation) equipped with a helium flow cryostat from Oxford Instruments for $YFe_2D_{4.2}$. Si or Ge powders were, respectively, used as internal standards for correcting the instrumental errors. The neutron powder diffraction (NPD) experiments were performed on $YFe_2D_{4.2}$ and $YFe_2(D_{0.36}H_{0.64})_{4.2}$ at the LLB (Saclay) using the G4.1 spectrometer with a wavelength of 2.4266 Å. The samples were contained in a vanadium sample holder. All the XRD and NPD patterns were refined with the Rietveld method, using the FULLPROF code.[15]

Differential Scanning Calorimetry (DSC) was performed in a TA-Q100 DSC apparatus from TA Instrument. The

TABLE I. Cell parameters of $YFe_2(D_{1-y}H_y)_{4.2}$ refined from the XRD patterns at 290 K. The values in brackets are the standard deviation on all the measured samples. p represents the cell parameter of the corresponding column.

y	a (Å)	b (Å)	c (Å)	β (°)	V (Å^3)
0	9.426(7)	5.734(4)	5.508(4)	122.39(4)	251.5(3)
0.64	9.439(7)	5.745(4)	5.517(1)	122.40(6)	252.7(7)
1	9.452(2)	5.751(2)	5.519(1)	122.35(2)	253.5(1)
$(p_H\text{-}p_D)/p_{D(\%)}$	0.26	0.28	0.19	−0.03	0.78

samples were placed in aluminum pans under a flowing purified argon atmosphere.

The magnetization measurements were performed using a SQUID magnetometer and a high-magnetic-field magnetometer ($B \leqslant 230$ kG) at the LCMI (Grenoble). The ^{57}Fe Mössbauer spectra were recorded between 4.2 and 300 K using a conventional constant acceleration-type spectrometer. The data were analyzed by superposing a set of discrete Lorentzians with equal width. The quadrupole interaction was treated as a perturbation to the magnetic hyperfine interaction. The isomer shift data are given relative to the source [Fe(Rh)], the difference to values given relative to α-Fe at room temperature being −0.12 mm/s.

III. RESULTS

A. X-ray and neutron diffraction

The XRD analysis at 290 K of several $YFe_2(H_yD_{1-y})_{4.2}$ ($y=0,0.64,1$) samples indicates that all samples crystallize in the same monoclinic structure described by the $C2/m$ space group, but with systematic increases of the cell parameters a,b,c and of the cell volume V vs y, whereas β remains constant within the error bars (Table I). This corresponds to a linear increase of 0.78% of the cell volume, as deuterium is replaced by hydrogen.

Since the magnetic transition occurs at low temperature, XRD patterns were measured above and below the transition for $YFe_2D_{4.2}$ and $YFe_2H_{4.2}$. At temperatures below the transition, the cell volumes are 252.5(2) Å^3 and 254.6(2) Å^3 for the deuteride and the hydride respectively, which corresponds to a difference of 0.83%, not very different from the one measured at room temperature. The change of volume at the transition $\Omega=(V-V_0)/V_0$, is larger for the deuteride ($\Omega=0.53\%$) than for the hydride ($\Omega=0.42\%$)).

The evolution of the cell parameters versus temperature has been also studied by NPD for $YFe_2D_{4.2}$ and $YFe_2(H_{0.64}D_{0.36})_{4.2}$. For the pure deuteride, due to the deuterium order, the NPD patterns should be refined in a primitive monoclinic cell with a doubling of the b parameter compared to the XRD cell.[13] For $YFe_2(H_{0.64}D_{0.36})_{4.2}$, the H/D contribution is cancelled due to the opposite value of the coherent scattering length b_n of the hydrogen and deuterium atoms [$b_n(H)=-3.74$ fm and $b_n(D)=6.67$ fm]. Therefore the $YFe_2(H_{0.64}D_{0.36})_{4.2}$ NPD patterns could be refined with only a contribution of the Y and Fe atoms in the same monoclinic cell than measured by XRD.

The refinement of the nuclear structure of $YFe_2D_{4.2}$ at 290 K is described in detail in Ref. 16. It was possible to refine the positions and the occupation numbers of the D atoms in a primitive monoclinic cell (space group $P21/a$), but without doubling the b parameter. In this description the Y and the three Fe sites occupy similar positions to those in the $C2/m$ space group, whereas 3.55(5) D atoms are located in 9 over 12 possible A2B2 sites and 0.55(5) D in 2 over 4 AB3 sites. The description of the cell in a superstructure with a doubling of the b parameter can be carried out in a monoclinic space group $P1c$ with 4 Y sites, 8 Fe sites, 48 A2B2 sites, and 16 AB3 sites. However, this means that the positions and occupancy factors for the 64 possible D atoms 256 parameters to refine have to be taken into account. Due to the small intensity of the superstructure lines, they cannot be resolved with a powder pattern. Nevertheless, the refinement in the simple monoclinic cell indicates that each Fe site is surrounded by a different number of deuterium atoms: 3.2(1) D for Fe1, 4.4(1) D for Fe2, and 5.2(1) D for Fe3. The Fe-D distances vary from 1.5 to 2.8 Å.

For clarity, in the following part and in the discussion we will consider the monoclinic unit cell defined by x-ray diffraction, i.e., without doubling the cell parameter along the b axis, as the "nuclear" cell.

The cell volume variation measured before and after the magnetovolumic transition by NPD is $\Omega=0.53\%$ for $YFe_2D_{4.2}$ and $\Omega=0.50\%$ for $YFe_2(H_{0.64}D_{0.36})_{4.2}$ (Fig. 1).

Concerning the magnetic structure, the NPD patterns of both $YFe_2D_{4.2}$ and $YFe_2(H_{0.64}D_{0.36})_{4.2}$ can be refined in a ferromagnetic structure between 1.4 K up to 80 and 100 K, respectively. The refinement of the NPD pattern of $YFe_2(H_{0.64}D_{0.36})_2$ indicates a progressive decrease of the Fe moment from 1.8(1) μ_B to 1.5(1) μ_B as the temperature increases from 1.4 to 100 K (Fig. 1). At the transition temperature the ferromagnetic line intensities decrease and additional antiferromagnetic (AF) reflections indexed with a $(0,1/4,0)$ propagation vector ($4b$) are observed for both compounds (Fig. 2). The intensity of the AF lines decreases until complete disappearance at $T_N=140$ and 160 K for $y=0$ and 0.64, respectively (Fig. 1). To refine the intensity of the AF lines, it is necessary to consider an AF coupling of the Fe moments belonging to the first and the third layer (one layer corresponds to the simple monoclinic cell observed by XRD). Above T_N a disordered state with a short-range magnetic order is probably present due to the strong background increase at a low angle.

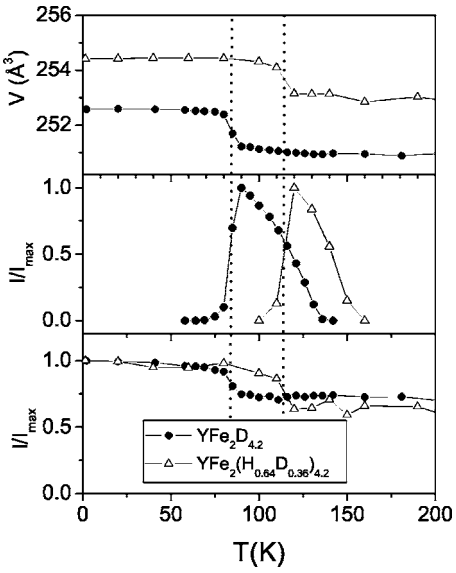

FIG. 1. Temperature evolution of V (top), the relative AF (middle) and F (bottom) line intensities (peaks marked in Fig. 2) refined from the NPD patterns of $YFe_2(H_yD_{1-y})_{4.2}$ ($y=0,0.64$) compounds. The dotted line indicates the positions of T_{M0} taken at the inflection point of the curves.

B. Differential scanning calorimetry

DSC experiments have been performed on $YFe_2H_{4.2}$. The transition temperature was found to be independent of the heating/cooling rate ranging from 1 K to 100 K/min. On heating, the transition temperature was found to be 132 ± 1 K, the hysteresis between heating and cooling being 3 K. The enthalpy of reaction was found to be 0.7(1) J/g.

C. Magnetization measurements

At 4.2 K all the compounds are ferromagnetically ordered. The spontaneous magnetization M_s extrapolated at $B=0$ increases from 1.86 to 2.06 μ_B/Fe between the deuteride and the hydride (Fig. 3). For all the $YFe_2(H_yD_{1-y})_{4.2}$ compounds M_S is smaller than in $YFe_2D_{3.5}$ ($M_S=2.15$ μ_B/Fe).

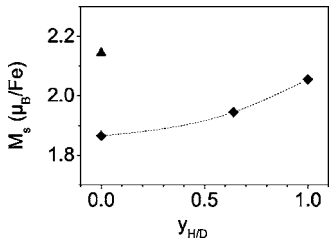

FIG. 3. Evolution of the mean Fe moment deduced from the spontaneous magnetization extrapolated at $B=0$ from magnetic curves measured up to 230 kG versus the hydrogen fraction y. The triangle corresponds to $YFe_2D_{3.5}$.

The magnetic isofields display a sharp decrease of the magnetization at a critical temperature $T_M(B,y)$ which depends on the applied field and the hydrogen fraction y (Fig. 4(a) for $y=1$). On the other hand, the magnetization isotherms display a field-induced behavior above $T_M(B,y)$, as shown in Fig. 4(b) for $y=1$. A linear variation of the transition field versus temperature determined at the inflection point is observed for the three compounds (Fig. 5). The extrapolation at $B=0$ leads to transition temperatures $T_M(B=0,y)$ denoted T_{M0}, in perfect agreement with those measured by neutron diffraction and DSC experiments. These values of T_{M0} are 84(2) K for $y=0$, 112(2) K for $y=0.64$ and 131(2) K for $y=1$.

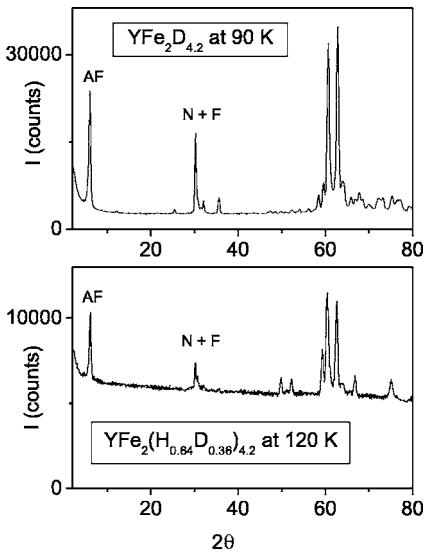

FIG. 2. A comparison of the NPD patterns of $YFe_2D_{4.2}$ at 90 K and $YFe_2(H_{0.64}D_{0.36})_{4.2}$ at 120 K.

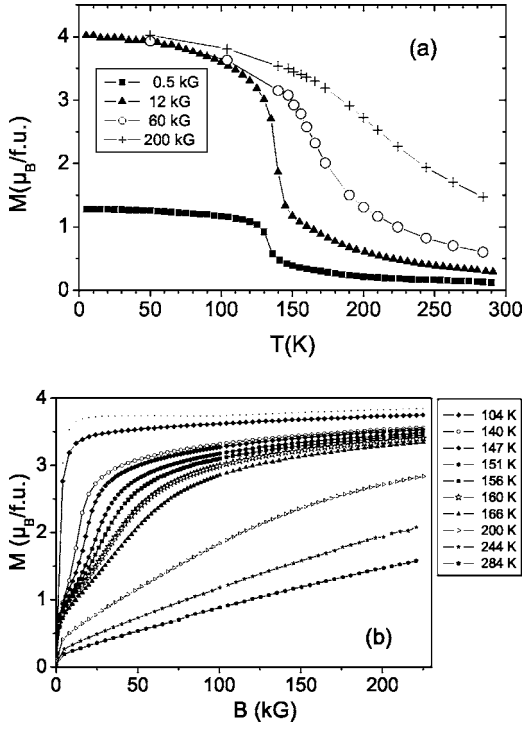

FIG. 4. Magnetization isofields (a) and isotherms (b) for $YFe_2H_{4.2}$.

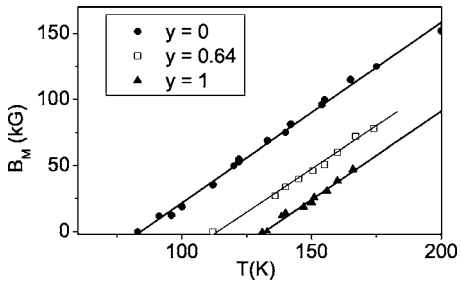

FIG. 5. Evolution of the transition field B_M versus temperature for the three $YFe_2(H_yD_{1-y})_{4.2}$ compounds.

The variation of $T_M(B,y)$-$T_{M0}(y)$ versus the transition field is independent of y, as shown in Fig. 6, and can be fitted with a linear equation,

$$T_M - T_{M0} = 1.7(7) + 0.71(1) * B, \quad (1)$$

with B given in kG.

The evolution of the temperature T_{M0} vs y is also linear according to

$$T_{M0} = 82.6(1) + 47.7(2) * y. \quad (2)$$

It may be noticed, albeit fortuitoulys, that the ratio of the transition temperature of the deuteride divided by the slope is equal to $\sqrt{3}$.

As the cell volume V_y measured at room temperature (RT) is proportional to y, a linear variation of the transition temperature T_0 vs V_y can be established (Fig. 7):

$$T_{M0} = -6327(5) + 25.5(2)V_y, \quad (3)$$

with V_y expressed in Å^3.

Room temperature (RT) rather than low-temperature cell volumes were used to plot $T_{M0}=f(V_y)$, since V_y at RT were measured in the same conditions using the same experimental device for all studied samples and should be more precise. A calculation with the low-temperature cell volume for $y=0$ and 1, leads to a slope of $\delta T_{M0}/\delta Vy = 22.5$ K/Å^3, not very different from the RT one.

D. Mössbauer experiments

The Mössbauer spectra of $YFe_2D_{4.2}$ (Ref. 16) and $YFe_2H_{4.2}$ (Fig. 8) show a similar shape but are shifted versus

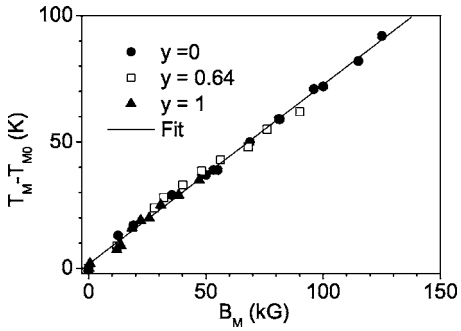

FIG. 6. Evolution of the difference between the transition temperatures T_M and T_{M0} versus the applied magnetic field.

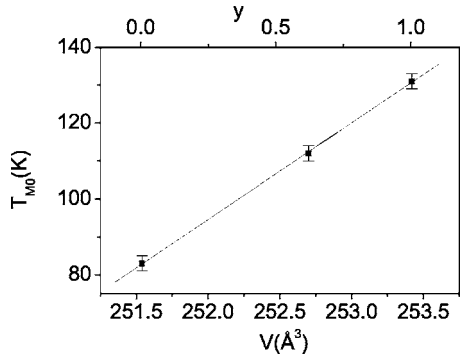

FIG. 7. Evolution of the transition temperature T_{M0} at $B=0$, versus the y H fraction (top scale) and the cell volume V_y (bottom scale).

temperature, in agreement with the magnetic measurements. Three different temperature regimes are observed: from 4.2 K to T_{M0}, the Mössbauer patterns can be fitted by superposing eight sextets with different hyperfine fields, isomer, and quadrupole shifts. Thus, it can fairly be supposed that all the Fe atoms carry a moment. Their hyperfine parameters, however, are influenced by the different local environment, particularly the ^{57}Fe hyperfine field.[17] Then, above T_{M0} and in the temperature range where the AF structure was observed by neutron diffraction, the Mössbauer spectra can be fitted by a mixture of sextets and doublets, both showing a wide distribution of hyperfine field and quadrupole shift, respectively.

In the third range, above the Néel temperature T_N, the Mössbauer spectra can be fitted with a superposition of eight doublets, demonstrating that the compound is already in the paramagnetic state (Fig. 8, $T=170$ K). The observed distri-

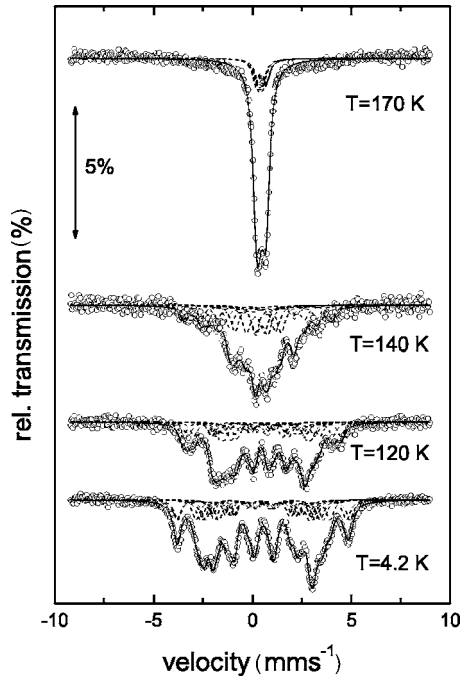

FIG. 8. Evolution of the ^{57}Fe Mössbauer spectra of $YFe_2H_{4.2}$ at selected temperatures.

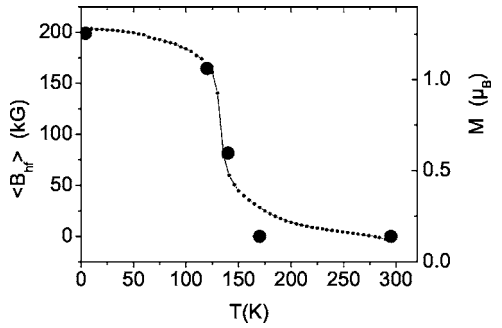

FIG. 9. A comparison of the mean hyperfine field (circles, left axis) and the isofield magnetization (dots, right axis) at 0.5 kG of $YFe_2H_{4.2}$.

bution of quadrupolar splitting and isomer shift can be related to the H(D) distribution around the different Fe atoms. The evolution of the hyperfine field which has been measured for selected temperatures is in agreement with the magnetization curve, as shown for $YFe_2H_{4.2}$ (Fig. 9).

IV. DISCUSSION

In this section we will discuss first the origin of the magnetovolumic transition, then the isotope effect, and finally the microscopic models concerning the itinerant electron metamagnetism (IEM) in relation to our results.

The origin of the magnetovolumic transition has been already been discussed in detail in Ref. 16 for $YFe_2D_{4.2}$, but for the sake of clarity in this paper these results will be summarized below. The lowering of the crystal symmetry from the cubic C15 to a monoclinic structure due to the deuterium order at low temperature leads to a splitting of the Fe site (96 g in the $Fd\bar{3}m$ space group) in three different Fe sublattices in the space group $C2/m$, denoted Fe1($2b$), Fe2($2c$) and Fe3($4e$) (Fig. 10). Because the three Fe sites have different numbers of D neighbors, their magnetic behaviors are not the same. The Fe3 site, which has about 5 D neighbors, is close to the instability of ferromagnetism, due to strong Fe–D bonding and the filling of its partial 3d band by additional D electrons. As a consequence, at T_{M0} the moment of the Fe3 is destabilized through an IEM mechanism, similar to that observed for Co in RCo_2 compounds.[18–28] The 0.53% volume change observed for $YFe_2D_{4.2}$ at the transition is close to the one found for $HoCo_2$ (IEM transition at

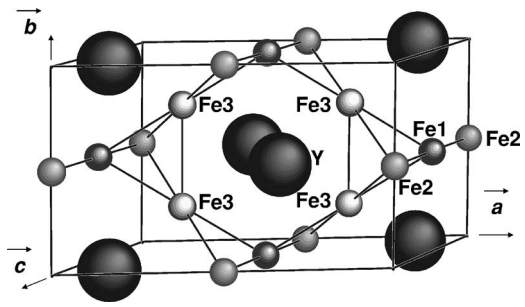

FIG. 10. Schematic representation of the monoclinic structure of $YFe_2(H,D)_{4.2}$. The D atoms have not been represented.

70 K).[19,20,29] The two remaining Fe1 and Fe2 sublattices still have an ordered moment, but due to the destabilization of the Fe3 moment, the direct exchange with the Fe3 atoms disappears. In the monoclinic structure the Fe1 and Fe2 atoms form chains separated from each other by about 5 Å, whereas the intrachain Fe–Fe distances is 2.75 Å. This means that ferromagnetic coupling can be maintained between the Fe moments belonging to the same chain, whereas an antiparallel coupling is observed between the chains. The variation of the sign of the coupling between the Fe moments might be related to the significant change of Fe–Fe interatomic distances from 2.75 to 5 Å. For example, it has been already observed in Fe–V or Fe–La superlattices that the sign of the inter-layer exchange coupling can be tuned from F to AF order or reversibly by changing the interlayer distances through H absorption in V or La layers.[30,33]

The lowering of the crystal symmetry in the monoclinic structure shows a particular distortion along the b axis: this parameter increases whereas the a and b parameters decrease as T decreases, and a doubling of the cell along the b axis is then necessary to index all the lines of the NPD patterns of $YFe_2D_{4.2}$ at a low temperature. This particular crystal structure influences the magnetic order, since the AF cell corresponds to four times the "nuclear" cell along the b axis. The evolution of the magnetic structure of $YFe_2D_{4.2}$ at $B=0$ as a function of temperature can therefore be summarized as follows: up to 75 K all the Fe atoms have a stable moment and the direct exchange interaction favors ferromagnetic ordering. At 75 K, the Fe3 atoms start to become destabilized and a progressive spin rearrangement of the Fe1 and Fe2 moments toward an AF coupling occurs up to 90 K. At 90 K, which corresponds to the maximum of the AF line, an AF magnetic coupling between the chains is achieved. Then, the Fe1 and Fe2 moments are continuously reduced, eventually vanishing at T_N (140 K). Above 140 K a short-range magnetic order remains very probably present. When a sufficient magnetic field is applied above the transition temperature T_M the Fe3 moments are again stabilized and the ferromagnetic order becomes more stable than the antiferromagnetic one.

Let us now examine the experimental data concerning the isotope effect. The x-ray diffraction measurements have shown that the a, b, and c cell parameters and then the cell volume V_y all increase from the pure deuteride to the pure hydride (Table I). This difference cannot be attributed to a larger H than D content in the hydride, since the amount of D or H atoms absorbed in all samples and measured by a volumetric method remains very close to 4.2. Larger cell parameters for hydrides compared to deuterides have already been observed for other compounds and is related to quantum effects: light atoms like hydrogen and its isotopes have a large amplitude of the zero-point vibration in their condensed phases. The root mean square amplitude of vibration of the hydrogen isotope in host metal is sensitive to the mass of hydrogen isotope and can vary from 0.19 Å for muons ($\mu+$), 0.25 Å for H, to 0.43 Å for T.[6] However, this large 0.8% cell volume difference between $YFe_2H_{4.2}$ and $YFe_2D_{4.2}$ is twice that of 0.4% observed between $YMn_2H_{4.2}$ (Ref. 31) and $YMn_2D_{4.2}$ (Ref. 32) and the role of secondary effects could not be eliminated.

The H for D substitution is also characterized by a larger spontaneous magnetization at 4.2 K, which is 1.86 μ_B/Fe for

the deuteride and 2.06 μ_B/Fe for the hydride. Since the Fe3 site is close to the ferromagnetic instability, this difference of 0.2 μ_B/Fe can be attributed to a lower Fe3 moment in the deuteride than in the hydride. On YFe_2H_x compounds ($x=0$, 3, 4, and 5), *ab initio* band structure calculations have clearly shown the competition between the cell volume increase that localizes the 3*d* band, thus increasing the Fe moments, and the electronic contribution of the H atoms that reduces the density of state (DOS) at the Fermi level (E_F) and consequently the magnitude of the Fe moment.[34] The calculations performed for YFe_2H_4, described in an orthorhombic structure, have confirmed a smaller Fe moment for one of the three Fe sites due to the difference of H neighbors. Therefore the larger volume of the hydride compared to the deuteride may be sufficient in the case where the width of the DOS strongly varies with the volume to induce a reduction of 0.4 μ_B on the Fe3 site, which contains 50% of the Fe atoms in the monoclinic cell. These calculations have also shown that in YFe_2H_5 the DOS at E_F is strongly reduced and that the non-spin-polarized configuration becomes more stable than the spin-polarized one since the Stoner criterium is not fullfilled. This means that the Fe moments are not stable in YFe_2H_5. These theoretical results indicate therefore that the limit of the ferromagnetic stability in YFe_2H_x hydrides is located between $x=4$ and 5.

The isotope substitution also strongly influences the magnetovolumic transition temperature T_{M0} that is shifted from 84 to 131 K as *y* changes from 0 to 1. The NPD, magnetization measurements, and Mössbauer experiments all indicate a reproducible, coherent, and systematic shift of the magnetic properties upon H/D substitution: the same type of magnetovolumic transition from a ferro to an antiferromagnetic structure (Figs. 1 and 2) and the same $\delta T/\delta B$ slope (Fig. 6). Here, also, it is worth examining how the difference of the cell volume can modify the thermal variation of the magnetic properties. For this purpose, we can compare the $YFe_2(H,D)_{4.2}$ compounds with other systems presenting an IEM behavior like the extensively studied RCo_2 compounds that have the same C15 cubic structure as YFe_2,[18–28] and like the $La(Fe_{1-x}Si_x)H_y$ series where the transition temperature was found very sensitive to the H content.[35–40]

In YCo_2 the metamagnetic transition occurs under 700 kG at 4.2 K.[21,22] The substitution of Co by a small amount of Al in YCo_2 allows a field transition decrease that is related to the cell volume increase according to $\delta B_M/\delta V=-57$ kG/Å^3.[41–44] In the case of $YFe_2(D_{1-y}H_y)_{4.2}$, combining Eqs. (1) and (3) leads to $\delta B_M/\delta V=-36$ kG/Å^3. It is of the same order of magnitude as in $Y(Co_{1-x}Al_x)_2$. On the contrary, a significant decrease of the transition temperature is observed when applying an external pressure on RCo_2 compounds, and therefore reducing the cell volume.[45]

Cubic $La(Fe_xSi_{1-x})_{13}H_y$ compounds are promising magnetic refrigerant materials due to a large magnetocaloric effect (MCE) associated with an IEM transition characterized by a variation of 1% of the cell volume.[35,37,39] For $La(Fe_{0.88}Si_{0.12})_{13}H_y$ the large MCE and IEM effects are preserved upon hydrogenation with an increase of the transition temperature from 200 to 278 K for an H content *y* varying from 0 to 1.1. In these compounds, the variation of the Curie temperature versus the room temperature cell volume leads to a variation $\delta T_C/\delta V$ of 4.4 K/Å^3. We can note that this value is five times smaller than in $YFe_2(D_{1-y}H_y)_{4.2}$, where $\delta T_M/\delta V=25.5$ K/Å^3. Such a difference is probably related to the fact that Fe in $YFe_2(D_{1-y}H_y)_{4.2}$ is closer to the ferromagnetic instability than in $La(Fe_{0.88}Si_{0.12})_{13}H_y$ compounds. This assumption is supported, for example, by the evolution of the Néel temperature versus the Mn–Mn distances measured in YMn_2 under pressure and in the corresponding hydrides, clearly showing a steeper increase of T_N near the onset of the Mn moment ($d_{Mn-Mn}=2.7$ Å) than for larger distances.[46]

In the above-mentioned compounds as well as in other systems that we will not describe here, it is clear that an increase of the cell volume stabilizes ferromagnetism and lowers either the critical field or the transition temperature.

At the microscopic scale several models have been developed to describe the IEM specific properties, which was first predicted by Wohlfarth and Rhodes using Landau's theory.[47] In their approach the IEM is related to a special shape of the DOS, with a strong positive curvature near the Fermi level that was attributed to the particular shape of the DOS due to 3*d*-5*d* hybridization effects.[48] However in this approach, the volume effects were not considered, although large volume increases are observed at the transition. Duc *et al.*[49] have then proposed a new approach to the IEM to show how this phenomenon results simply from the interplay between magnetic and elastic energy in magnetic systems close to the critical conditions for the appearance of ferromagnetism.

The total energy E_{tot} is found to be a function of Ω for different values of the band filling, with and without an applied field. The $E_{tot}(\Omega)$ curves show a second energy minimum, the position of which can be either above or below the energy of the paramagnetic state ($\Omega=0$) depending on the filling of the conduction band, the external field or the applied pressure. It is noticeable that the shape of these $E_{tot}(\Omega)$ curves are quite similar to the variations of the $E_{tot}(B)$ obtained for different applied fields by Wohlfarth and Rhodes.[47]

In addition, the *ab initio* band structure calculations on YFe_2H_x compounds have shown that the critical value for the appearance of ferromagnetism is located between $x=4$ and 5 and that their magnetic properties result from a competition between the cell volume increase and the H electron concentration.[34] These calculations also indicate that for these H concentrations the Fermi level in located in a range were the DOS decreases steeply as the energy increases (see Fig. 7 in Ref. 34). Therefore a small volume variation can be responsible of a significant change of the DOS at E_F.

Considering the observed properties of several materials, the model developed by Duc *et al.*[49] and the YFe_2H_x *ab initio* calculations,[34] there exists a large presumption that the strong influence of the H/D isotope substitution observed on the magnetic properties of the $YFe_2(H,D)_{4.2}$ system is also related to the large volume difference between the samples. The transition temperature may also be affected by a difference of hydrogen and deuterium distribution around the Fe3 atoms, responsible for the IEM transition. It is difficult to precisely determine whether the H and D atoms occupy exactly the same positions with the same occupancy factors in

these compounds. NPD experiments have not been performed yet on $YFe_2H_{4.2}$, but due to the large neutron incoherent scattering of hydrogen atoms the signal/noise ratio of the corresponding NPD pattern will be much smaller than in the deuteride, and it would be even more difficult to solve fully the structure. Nevertheless, if such an effect exists we believe that it is rather small compared to the volume effect. We have synthesized several samples with pure H, pure D, or a mixture of both, which could show some small variations of the H or D content. We have concluded that the transition temperature is not at all sensitive to the sample preparation, but only to the nature of the isotope. The linearity of T_{M0} versus the cell volume, would also be difficult to explain without the important role of the volume. However to get a better understanding of this large isotope effect and, in particular, its relation with the cell volume, neutron experiments under pressure as well as chemical substitutions of Y by rare earth are now currently under progress.

V. CONCLUSIONS

This work has confirmed the large isotope effect on the structural and magnetic properties of the $YFe_2(H_yD_{1-y})_{4.2}$ compounds. The H for D substitution leads to a significant cell volume increase attributed partially to the isotope mass influence at the zero-point vibration. An increase of the saturation magnetization at 4.2 K and a linear relationship between the transition temperature T_{M0} and both y and the cell volume of the $YFe_2(H_yD_{1-y})_{4.2}$ compounds have been observed upon H for D substitution. This isotope effect on the magnetic properties has been explained by the volume difference between the hydride and the deuteride, since volume effects have a strong influence on the magnetic properties of IEM compounds. This particular behavior deserves further experimental and theoretical studies in order to get a better understanding of the influence of hydrogen on the Fe moment near the instability of ferromagnetism.

ACKNOWLEDGMENTS

We are thankful to V. Lalanne (LCMTR, France) for his help in the sample preparation and to E. Leroy (LCMTR, France) for an EPMA analysis. We want to thank A. Linbaum (Tu Vienna), M. Latroche, and O. Rouleau (LCMTR, France) for their help in performing x-ray diffraction measurements at a low temperature. Neutron diffraction experiments were achieved thanks to the allocated beam time at the Léon Brillouin Laboratory and magnetization up to 230 kG thanks to the measuring time at the High Magnetic Field Laboratory.

*Corresponding author. Electronic address: paulbon@glvt-cnrs.fr

[1] R. Lässer and K.-H. Klatt, Phys. Rev. B **28**, 748 (1983).
[2] B. Andreyev, V. Shitikov, E. Magomedbekov, and A. Shafiev, J. Less-Common Met. **90**, 161 (1983).
[3] Y. Naik, G. A. Rama Rao, and V. Venugopal, Intermetallics **9**, 309 (2001).
[4] M. Shuai, Y. Su, Z. Wang, P. Zhao, J. Zou, and S. Wu, J. Nucl. Mater. **301**, 203 (2002).
[5] S.-W. Cho, E. Akiba, Y. Nakamura, and H. Enoki, J. Alloys Compd. **297**, 253 (2000).
[6] P. Jena and C. B. Satterthwaite, in *Materials Research Society, Symposia Proceedings*, edited by Kaufmann, and G. K. Shenoy (Elsevier North-Holland, Inc., Amsterdam, 1981), Vol. 3, p. 547.
[7] P. Jena, C. L. Wiley, and F. Y. Fradin, Phys. Rev. B **40**, 578 (1978).
[8] E. Wicke, H. Brodowsky, and H. Züchner, in *Hydrogen in Metals II Applications—Oriented Properties*, Vol. 29, edited by G. Alefeld and J. Völkl (Springer-Verlag, Berlin, 1978), p. 73.
[9] P. Vajda, in *Handbook on the Physics and Chemistry of Rare Earths*, edited by K. A. Gschneidner, Jr., and L. R. Eyring (Elsevier Science B. V., Amsterdam, 1995), Vol. 20, p. 207.
[10] L. H. Nosanow, Phys. Rev. **146**, 120 (1966).
[11] P. Jena, F. Y. Fradin, and D. E. Ellis, Phys. Rev. B **20**, 3543 (1979).
[12] H. Kronmuller, in *Hydrogen in Metals I, Basic Properties*, edited by G. Alefeld and J. Völkl (Springer-Verlag, Berlin, 1978), Vol. 28, p. 289.
[13] V. D. Kodibagkar, P. A. Fedders, C. D. Browning, R. C. Bowman, Jr., N. L. Adolphi, and M. S. Conradi, Phys. Rev. B **67**, 045107 (2003).
[14] V. Paul-Boncour, G. André, F. Bourée, M. Guillot, G. Wiesinger, and A. Percheron-Guégan, Physica B **350**, e27 (2004).
[15] J. Rodríguez-Carvajal, in *Congr. Int. Union of Crystallography*, Toulouse, France, 1990, p. 127.
[16] V. Paul-Boncour, M. Guillot, G. André, F. Bourée, G. Wiesinger, and A. Percheron-Guégan, J. Alloys Compd. **404–406C**, 335 (2005).
[17] G. Wiesinger, V. Paul-Boncour, S. M. Filipek, C. Reichl, I. Marchuk, and A. Percheron-Guégan, J. Phys.: Condens. Matter **17**, 893 (2005).
[18] W. Dunhui, T. Shaolong, H. Songling, S. Zhenghua, H. Zhida, and D. Youwei, J. Alloys Compd. **360**, 11 (2003).
[19] D. Gignoux, D. Givord, and J. Schweizer, J. Phys. F: Met. Phys. **7**, 1823 (1977).
[20] F. Givord and J. S. Shah, C. R. Séances Acad. Sc. Paris, Ser. B **274**, 923 (1972).
[21] T. Goto, K. Fukamichi, T. Sakakibara, and H. Komatsu, Solid State Commun. **72**, 945 (1989).
[22] T. Goto, T. Sakakibara, K. Murata, H. Komatsu, and K. Fukamichi, J. Magn. Magn. Mater. **90–91**, 700 (1990).
[23] E. Gratz and A. S. Markosyan, J. Phys.: Condens. Matter **13**, R385 (2001).
[24] K. Hataway and J. Cullen, J. Phys.: Condens. Matter **3**, 8911 (1991).
[25] K. Schwarz and P. Mohn, J. Phys. F: Met. Phys. **14**, L129 (1984).
[26] H. Yamada and M. Shimizu, J. Phys. F: Met. Phys. **15**, L175 (1985).
[27] H. Yamada, T. Tohyama, and M. Shimizu, J. Magn. Magn. Mater. **66**, 409 (1987).
[28] H. Yamada, T. Tohyama, and M. Shimizu, J. Phys. F: Met. Phys.

17, L163 (1987).
[29] F. Givord, R. Lemaire, and J. S. Shah, C. R. Séances Acad. Sc. Paris, Ser. B **274**, 161 (1972).
[30] B. Hjorvarsson, C. Chacon, H. Zabel, and V. Leiner, J. Alloys Compd. **356–357**, 160 (2003).
[31] J. Przewoznik, V. Paul-Boncour, M. Latroche, and A. Percheron-Guégan, J. Alloys Compd. **225**, 436 (1995).
[32] M. Latroche, V. Paul-Boncour, A. Percheron-Guégan, and F. Bourée-Vigneron, J. Alloys Compd. **274**, 59 (1998).
[33] W. Lohstroh, F. Leuenberger, W. Felsch, H. Fritzsche, and H. Maletta, J. Magn. Magn. Mater. **237**, 77 (2001).
[34] V. Paul-Boncour and S. F. Matar, Phys. Rev. B **70**, 184435 (2004).
[35] S. Fujieda, A. Fujita, K. Fukamichi, Y. Yamazaki, and Y. Iijima, Appl. Phys. Lett. **79**, 653 (2001).
[36] S. Fujieda, A. Fujita, and K. Fukamichi, Appl. Phys. Lett. **81**, 1276 (2002).
[37] A. Fujita, Y. Akamatsu, and K. Fukamichi, J. Appl. Phys. **85**, 4756 (1999).
[38] A. Fujita, S. Fujieda, K. Fukamichi, H. Mitamura, and T. Goto, Phys. Rev. B **65**, 014410(1) (2001).
[39] A. Fujita, S. Fujieda, Y. Hasegawa, and K. Fukamichi, Phys. Rev. B **67**, 104416 (2003).
[40] S. Fujitani, I. Yonezu, N. Furukawa, E. Akiba, H. Hayakawa, and S. Ono, J. Less-Common Met. **172–174**, 220 (1991).
[41] K. Yoshimura and Y. Nakamura, Solid State Commun. **56**, 767 (1985).
[42] H. Wada, K. Yoshimura, G. Kido, M. Shiga, M. Mekata, and Y. Nakamura, Solid State Commun. **65**, 23 (1988).
[43] T. Goto, A. Katori, T. Sakakibara, H. Mitamura, K. Fukamichi, and K. Murata, J. Appl. Phys. **76**, 6682 (1994).
[44] T. Goto and M. I. Bartashevich, Physica B **246–247**, 495 (1998).
[45] O. Syshchenko, T. Fujita, V. Sechovsky, M. Divis, and H. Fujii, J. Magn. Magn. Mater. **226–330**, 1062 (2001).
[46] V. Paul-Boncour, J. Alloys Compd. **367**, 185 (2004).
[47] E. P. Wohlfarth and P. Rhodes, Philos. Mag. B **7**, 1817 (1962).
[48] M. Cyrot, D. Gignoux, F. Givord, and M. Lavagna, J. Phys. C **40**, 171 (1979).
[49] N. H. Duc, D. Givord, C. Lacroix, and C. Pinettes, Europhys. Lett. **20**, 47 (1992).